

Cu(2) nuclear resonance evidence for an original magnetic phase in aged 60K-superconductors $\text{RBa}_2\text{Cu}_3\text{O}_{6+x}$ ($\text{R}=\text{Tm}, \text{Y}$)

A.V.Dooglav^{1,2}, H.Alloul², O.N.Bakharov^{1,3}, C.Berthier³, A.V.Egorov^{1,4}, M.Horvatic³, E.V.Krjukov¹, P.Mendels², Yu.A.Sakhratov¹, M.A.Teplov¹

¹*Magnetic Resonance Laboratory, Kazan State University, 420008 Kazan, Russia*

²*Laboratoire de Physique des Solides, Université de Paris-Sud, 91405 Orsay Cedex, France*

³*Grenoble High Magnetic Field Laboratory, Max-Planck Institut für Festkörperforschung and Centre National de la Recherche Scientifique, BP 166, 38042 Grenoble Cedex 9, France*

Laboratoire de Spectrométrie Physique, Université Joseph Fourier, Grenoble 1, 38402 Saint-Martin d'Hères Cedex, France

⁴*KFA Forschungszentrum Jülich, IFF, D-52425 Jülich, Germany*

It is widely believed that the long-range antiferromagnetic order in the $\text{RBa}_2\text{Cu}_3\text{O}_{6+x}$ compounds ($\text{R}=\text{Y}$ and rare earths except of Ce, Pr, Tb) is totally suppressed for the oxygen index $x \geq 0.4$ (AFM insulator-metal transition). We present the results of the copper NQR/NMR studies of aged $\text{RBa}_2\text{Cu}_3\text{O}_{6+x}$ ($\text{R}=\text{Tm}, \text{Y}$) samples showing that a magnetic order can still be present at oxygen contents x up to at least 0.7 and at temperatures as high as 77K.

I. INTRODUCTION

An enormous amount of papers, both experimental and theoretical, are devoted to the NMR and NQR studies of copper in superconducting $\text{YBa}_2\text{Cu}_3\text{O}_{6+x}$ layered cuprates. It is considered well known that in non-superconducting materials ($x < 0.4$) nuclei of copper located in the CuO_2 planes experience the influence of a strong internal magnetic field $H_{int} \approx 80$ kOe which is perpendicular to the c -axis, and that in superconductors ($x > 0.4$) such field is absent and $^{63,65}\text{Cu}(2)$ nuclei with the spin $I = 3/2$ give typical NQR spectra at frequencies of $\nu_Q \approx 25 \div 32$ MHz, i.e., in the same frequency range as that for NQR spectra of two-fold coordinated "chain" copper $^{63,65}\text{Cu}(1)$ ¹. While studying NMR of thulium in oxygen-deficient $\text{TmBa}_2\text{Cu}_3\text{O}_{6+x}$ compounds² we have discovered the wide and subtle absorption line (Fig.1) which looked like copper NMR line but could not have been attributed to the mentioned Cu(2) and Cu(1) centers with $\nu_Q \approx 25 \div 32$ MHz and $H_{int} = 0$. We consequently undertook experiments with $\text{TmBa}_2\text{Cu}_3\text{O}_{6+x}$ samples ($x = 0.51, 0.6, 0.7$) in zero external field at $T=4.2\text{K}$, which allowed us to observe a Cu(2) ZFNMR spectrum completely different from those described in the literature. The results of these experiments are presented in this paper. The analysis of Cu(2) spectra of both types corresponding to $H_{int} \neq 0$ (type *I*, $\nu_{ZFNMR} = 55 - 135$ MHz) and $H_{int} = 0$ (type *II*, $\nu_Q \approx 25 \div 32$ MHz) shows that each of them belongs to two varieties of Cu(2) centers, *A* and *B*, possessing different NQR frequencies and that A_I - and B_I -centers differ much in the value of H_{int} . Similar results are obtained for one $\text{YBa}_2\text{Cu}_3\text{O}_{6.66}$ sample³.

II. EXPERIMENTAL

The $\text{TmBa}_2\text{Cu}_3\text{O}_{6+x}$ samples used in these experiments were c -axis-oriented powders mixed with paraffin (hereafter denoted as $\text{Tm}6+x$). They were previously used for Tm NMR studies². All of them were stored at room temperature for almost 6 years after preparation. Critical temperatures ($T_c^{onset}=53\text{K}, 61\text{K}$ and 64K for $x = 0.51, 0.6$ and 0.7 , respectively) were obtained from measurements of the diamagnetic susceptibility at a frequency of 1 kHz. Home-built spin-echo NQR spectrometers were used for the Cu(2) NQR and ZFNMR measurements. Examples of the copper NQR spectra in $\text{Tm}6.6$ are shown in Fig.2. Comparing the non-saturated (NS) and saturated (S) spectra (Figs.2a,b) taken at 4.2K with pulse sequence repetition rates of 1 and 200 Hz, respectively, one can distinguish two contributions with different spin-lattice relaxation times T_1 (Fig.2c) and separate them (Figs.2d,e) by using a simple subtraction procedure. Two narrow lines in Fig.2e corresponding to the long T_1 time are believed to originate from the two-fold coordinated $\text{Cu}(1)_2$ sites which belong to "empty chains" surrounded by "full chains" in the CuO_x plane¹. The broad spectrum in Fig.2d characterized by the short T_1 has a two-hump shape typical for the Cu(2) NQR spectrum of an annealed sample⁴. In the following it is denoted as the spectrum of type *II*. Computer simulations have shown that this two-hump spectrum can be described by a sum of four Gaussians (two sites, A_{II} and B_{II} , times two isotopes,

^{63}Cu and ^{65}Cu), the amounts of A_{II} - and B_{II} -sites appearing in a ratio of approximately 2:1 independent of the oxygen index x . The parameters of the spectra taken with a fixed pulse separation time $\tau = 25\mu\text{s}$ are given in Table I for three samples studied.

The Cu(2) ZFNMR (type *I*) spectra taken at 4.2K with a fixed pulse separation time $\tau = 33\mu\text{s}$ are shown in Fig.3. A similar spectrum was observed in Tm6.6 at a temperature of 77K (shown by filled squares in Fig.3b). It should be noted here that in our experiments the well pronounced spectra of type *I* were observed only in those Tm- and Y-compounds which exhibited well pronounced two-hump spectra of type *II* (Fig.2d). An obvious downfall of the spectral intensity at around 98 MHz which looks particularly pronounced at $x=0.7$ clearly shows that the ZFNMR spectrum is also composed of two contributions, those are the low-frequency fragment (LFF) at 55-98 MHz and the high-frequency fragment (HFF) at 98-135 MHz.

In order to estimate the integrated intensities, S_I and S_{II} , of the ZFNMR (type *I*) and NQR (type *II*) spectra, we have corrected them according to the spin-spin relaxation times T_2 measured at the main peaks of the spectra. All spin-echo decays measured at 4.2K have been found to obey the following formula: $A_{2\tau}/A_0 = \exp(-(2\tau/T_2)^n)$. In the series of Tm compounds, the longest T_2 -times were measured for the Tm6.6 sample: $T_2=72, 64, 119, 75, 43$ and $54 \mu\text{s}$ at frequencies of 62, 74, 87, 109, 116 and 124 MHz, respectively; the values of n were found to lie in the range 0.7-0.9. Because of the broad frequency range the echo intensity has also been corrected by a factor ν^2 , one factor ν due to the nuclear magnetization, the other one due to the precession frequency of the nuclear magnetization. The T_2 -correction procedure consisted of four steps: (i) fitting the experimental Cu(2) spectra by a superposition of Gaussians (6 for type *I* and 4 for type *II*); (ii) multiplying intensity of each component by the corresponding factor $\exp((2\tau/T_2)^n)$; (iii) summation of the corrected Gaussian lines; (iv) ν^2 correction. The resulting spectra are shown by solid lines in Fig.4. The results of the best fit for the Tm6.51 and Tm6.6 samples show the LFF- and HFF-intensities to be in a ratio $\approx 2 : 1$ which allows us to ascribe them, in analogy with the above *II*-type spectrum, to the A_I - and B_I -sites, respectively. In Table II, the partial ratios S_{AI}/S_{BI} and S_{AII}/S_{BII} for spectral intensities of the A - and B -sites are given along with the ratio S_{II}/S_I . The absolute values of the signal intensities per 1 gram of material, S_I and S_{II} , shown in the last column of Table II, are normalized to the intensity of the "ordinary" Cu(2) ZFNMR spectrum of the $\text{TmBa}_2\text{Cu}_3\text{O}_{6.1}$ antiferromagnet as observed at $T=4.2\text{K}$ in the frequency range from 61 to 123 MHz.

As can be seen from the last column of Table II, the volume fraction of the material contributing to the total Cu(2) resonance absorption varies from sample to sample being equal to 1.00, 0.58 and 0.83 in Tm6.51, Tm6.6 and Tm6.7, respectively, as compared to Tm6.1. Since the Cu(2) ZFNMR spectrum is certainly produced by a non-superconductor, the question arises: What part of the Cu(2) NQR signal intensity can be attributed to the superconducting fraction? To answer this question, we have re-measured the ac diamagnetic susceptibility of the Tm6+x samples ($x=0.51 \div 1.0$)² at a temperature of 4.2 K. The results of the measurements (see inset in Fig.1) clearly show that the superconducting fraction decreases with ageing time (with no changes in T_c), the tendency being most pronounced for the 60K-superconductors, and that the superconducting fraction of the 6-years old samples under study is quite small, i.e., 0.05, 0.05 and 0.15 for Tm6.51, Tm6.6 and Tm6.7, respectively. Comparing the latter quantities with the Cu(2) NQR signal intensities (0.79, 0.42 and 0.73, respectively), one arrives at the conclusion that at least a part of the Cu(2) absorption observed at 4.2K definitely originates from the non-superconducting material. This conclusion is also supported by the fact that in one of the samples studied, $\text{YBa}_2\text{Cu}_3\text{O}_{6.66}$, which was prepared quite recently, we did not observe a two-hump NQR, nor a ZFNMR spectrum³.

III. DISCUSSION

In order to clarify the origin of the LFF- and HFF-spectra, we have tried to fit the Cu(2) ZFNMR in a correct way assuming that the A_I - and B_I -sites can be characterized by different values of ν_Q , H_{int} and θ (angle between \mathbf{H}_{int} and the c -axis). Prior to fitting the experimental spectra (Fig.3) have been T_2 -corrected by the function $f(\nu) = F_0(\nu)/F_{2\tau}(\nu)$, where $F_{2\tau}(\nu)$ is the ZFNMR spectrum shown in Fig.4 by a dotted line, and $F_0(\nu)$ is the spectrum represented by a solid line. The spectra of Tm6.51 and Tm6.6 corrected in this way are shown in Fig.5. The fitting procedure included numeric diagonalization of the two Hamiltonians and calculation of all the transitions probabilities ($\sim \nu^2$). When calculating averaged values of the probabilities in oriented powdered samples, we have taken an orientation of a radiofrequency field with respect to the c -axis into account ($\mathbf{H}_1 \perp c$). In all the cases considered, the Lorentzian shape of an individual resonance line was found to fit the experimental data much better than the Gaussian one. Two versions of the fit have been considered. When the angles θ were allowed to be free, the best fit of the Cu(2) ZFNMR spectrum of Tm6.51 was obtained at the following parameters (see solid line in Fig.5a):

$$\begin{aligned} & \text{"}\theta \text{ free"} \\ & A_I\text{-sites, } \nu = 55 - 98 \text{ MHz, intensity } S_{AI} = 62(6)\%, \\ & \theta = 82(4)^\circ, H_{int} = 63.9(3) \text{ kOe, } \nu_Q = 31(2) \text{ MHz,} \end{aligned} \quad (1)$$

$$\begin{aligned}
& B_I\text{-sites, } \nu = 98 - 127 \text{ MHz}^5, \text{ intensity } S_{BI} = 38(3)\%, \\
& \theta = 64(1)^\circ, H_{int} = 97.7(2) \text{ kOe}, \nu_Q = 25(2) \text{ MHz}, \\
& \text{linewidth } FWHM = 4.4(4) \text{ MHz}.
\end{aligned} \tag{2}$$

The corresponding parameters for the Tm6.6 sample have been obtained as follows (Fig.5b):

$$\begin{aligned}
& A_I\text{-sites, } \nu = 55 - 98 \text{ MHz}, S_{AI} = 66(4)\%, \\
& \theta = 83(3)^\circ, H_{int} = 64.1(2) \text{ kOe}, \nu_Q = 30(1) \text{ MHz},
\end{aligned} \tag{3}$$

$$\begin{aligned}
& B_I\text{-sites, } \nu = 98 - 127 \text{ MHz}^5, S_{BI} = 34(2)\%, \\
& \theta = 63.5(5)^\circ, H_{int} = 97.6(1) \text{ kOe}, \nu_Q = 27(1) \text{ MHz}, \\
& FWHM = 4.4(3) \text{ MHz}.
\end{aligned} \tag{4}$$

In the second version ($\theta = 90^\circ$) both internal fields were assumed to lie in the ab plane. The results of this fit for Tm6.6 are as follows (see solid line in Fig.5c):

$$\begin{aligned}
& \text{''}\theta = 90^\circ\text{''}^* \\
& A_I\text{-sites, } \nu = 55 - 98 \text{ MHz, intensity } S_{AI} = 66(6)\%, \\
& H_{int} = 64 \text{ kOe}^*, \nu_Q = 30 \text{ MHz}^*,
\end{aligned} \tag{5}$$

$$\begin{aligned}
& B_I\text{-sites, } \nu = 98 - 135 \text{ MHz}, S_{BI} = 34(3)\%, \\
& H_{int} = 103 \text{ kOe}^*, \nu_Q = 15.3(7) \text{ MHz}, \\
& FWHM = 4.8(4) \text{ MHz}
\end{aligned} \tag{6}$$

(* denotes the fixed parameters). The second fit seems to agree with experiment worse than the first one, but this can be due to incorrect intensities of the HFF-lines deduced from the T_2 -correction procedure. We believe that at the present stage both versions can be considered satisfactory; more experimental work is needed to make a choice between them. In both cases the Cu(2) NMR line in Fig.1 has been identified as originating from two groups of A_I -lines (at 58-63 MHz and 74-79 MHz).

Then summarizing all experimental facts, one should adopt that at least a part of the two-hump NQR spectrum, which is supposed to be typical for the annealed 123 superconductors with high T_c s⁴, and the ZFNMR spectrum, which is observed in the 60K-superconductors exhibiting a well pronounced two-hump NQR, are actually representing a non-superconducting material. In what follows, we try to speculate about the plausible structure of this material. It is known that a structural (chemical) micro-phase separation takes place in the oxygen-deficient 123 superconductors^{2,6-9}. Therefore, one could naturally expect to find the defects of the crystal lattice in the form of layers (reflecting the basic property of the layered structure itself) and, following this way, could associate the two types of Cu(2) spectra with two different non-superconducting micro-phases, i.e., hole doped (type II) and non-doped (type I) layers, forming some kind of stacking sequence along the c -axis². On the other hand, the coincidence of the ν_Q -values (see Eqs.(1)-(4) and Table I) in the two absolutely different phases lead us to consider that both types of Cu(2) spectra might originate from the same CuO_2 layers (bilayers).

To make a choice between these two scenarios, one should use the neutron scattering data which gives a direct information on a magnetic structure of the oxygen-deficient 123 compounds. The thorough studies of the neutron scattering in $\text{YBa}_2\text{Cu}_3\text{O}_{6.6}$ ¹⁰⁻¹³ have resulted in a recent observation¹³ of incommensurate magnetic fluctuations peaked at $\vec{Q} = (1/2 \pm \delta, 1/2 \pm \delta)$ with $\delta = 0.057 \pm 0.006$ r.l.u. It was also found that the dynamical susceptibility $\chi''(\vec{q}, \omega)$ at the incommensurate positions first appears at temperatures somewhat above T_c and then increases on cooling below T_c , altogether with the suppression of magnetic fluctuations at the commensurate points. These observations look similar to those for the $\text{La}_{1.6-x}\text{Nd}_{0.4}\text{Sr}_x\text{CuO}_4$ compounds^{14,15} and thus can be considered as giving evidence for a formation of a static (or quasi-static) stripe pattern in the CuO_2 layers. The layer-by-layer separation scenario seems to be inconsistent with such a stripe model. On the contrary, the stripe-like modulation of charge and spin densities in CuO_2 layers resulting in an inequivalency of Cu(2) sites looks very likely. Indeed, analyzing the data of Table II, one can conclude that there could exist a certain value of x_{pin} (close to 0.6) which corresponds to the following relations:

$$S_{AI}/S_{BI} = 2, \quad S_{AII}/S_{BII} = 2, \quad S_{II}/S_I = 2. \tag{7}$$

These relations can be understood in the frame of the charge stripe model suggested in¹⁶. A plausible stripe pattern corresponding to the optimally doped CuO_2 planes (1/6 hole per CuO_2 unit) is shown in Fig.6a. If one takes every

third stripe away (Fig.6b), the hole concentration p becomes $(2/3) \times (1/6) = 1/9$. According to the empirical formula $p = 0.187 - 0.21(1 - x)$, suggested by Tallon et al.¹⁷ for $x \geq 0.45$, the concentration $p = 1/9$ corresponds to $x = 0.64$ which is close to what is expected for Eq.(7) to hold. The magnetic superstructure shown in Fig.6b has a period of 18 lattice spacings. This period and the diagonal direction [110] of the stripes in Fig.6b exactly corresponds to the incommensurate magnetic fluctuations observed in $\text{YBa}_2\text{Cu}_3\text{O}_{6.6}$ ¹³: the model in Fig.6b predicts incommensurate peaks at $\vec{Q} = (1/2 \pm \delta, 1/2 \pm \delta)$ with $\delta = 1/18 = 0.0556$. In this stripe pattern, it is easy to distinguish four different Cu(2) sites which could be identified as sites A_I (at borders of magnetic stripes), B_I (at centers of magnetic stripes), A_{II} (at borders of non-magnetic stripes), B_{II} (at centers of non-magnetic stripes). An alternative possibility is to ascribe the B_{II} -sites to copper atoms located at outer borders of the non-magnetic bi-stripes allowing the A_{II} -sites to occupy four lines of coppers inside the bi-stripes. In any case, however, one has a problem to explain why the transferred hyperfine field from the A_I -copper spins does not influence the NQR spectrum of the neighboring type-II copper centers. Further experimental work is necessary to better understand the allocation of the Cu(2) centers responsible for the two-hump NQR spectrum.

It is known that the observation of the static stripe-phase order of holes and spins in $\text{La}_{1.6-x}\text{Nd}_{0.4}\text{Sr}_x\text{CuO}_4$ ^{14,15} has appeared possible due to pinning of the stripes by the neodymium impurities. What could be the reason for stripes to be pinned in non-stoichiometric 123 compounds? We believe that the so-called "OrthoIII" superstructure in CuO_x planes could cause pinning of charge stripes in CuO_2 planes since this superstructure has a period ($3a_0$) commensurate with the period of the stripe pattern shown in Fig.6b. A possibility for the OrthoIII to form a stable phase at $x = 0.65 - 0.77$ was proved by the electron¹⁸, X-ray and neutron¹⁹ diffraction measurements. The above oxygen contents appear to be shifted to higher values than that (x_{pin}) expected for the condition Eq.(7) to be fulfilled. However, the value of x_{pin} may happen to result from an interplay between the OrthoIII ordering of CuO_x layers at $x > x_{pin}$ and an appropriate hole doping of CuO_2 layers ($p = 1/9$ per CuO_2 at $x < x_{pin}$). Experiments with an $\text{YBa}_2\text{Cu}_3\text{O}_{6.77}$ single crystal¹⁹ have shown that the OrthoIII phase is stable at temperatures below 75°C. Therefore, the interactions responsible for the formation of the OrthoIII phase seem to be rather weak and can be easily disturbed by thermally-activated oxygen diffusion. This feature of the T-x phase diagram allows us to understand why the Cu(2) ZFNMR was observed in our experiments only in those 123 superconductors which were subjected to a very long-term room-temperature annealing.

IV. CONCLUSIONS

The Cu(2) nuclear resonance spectra were studied at liquid helium temperatures in samples of oxygen-deficient 60K-superconductors, $\text{TmBa}_2\text{Cu}_3\text{O}_{6+x}$ and $\text{YBa}_2\text{Cu}_3\text{O}_{6.66}$, stored at room temperature for a long time (up to 6 years). Cu(2) ZFNMR spectra different from those known so far were observed, indicating the presence of a non-superconducting phase in the superconducting samples. The quantitative analysis of the copper resonance absorption intensities in different samples lead us to consider that both types of Cu(2) spectra (ZFNMR at 55-135 MHz and at least a part of NQR at 25-32 MHz) might originate from the same non-superconducting CuO_2 layers decorated by the pinned charge stripes.

V. ACKNOWLEDGEMENTS

This work was supported in part by the Russian Scientific Council on Superconductivity, under Project 94029, by the Russian Foundation for Basic Research, under Project 96-02-17058a, by the NATO Scientific and Environmental Affairs Division, under Grant HTEC.LG-950536, and by the INTAS, under Grant 96-0393.

¹ I.Heinmaa, H.Lütgemeier, S.Pekker, G.Krabbes, and M.Buchgeister, Appl.Magn.Reson. **3**, 689 (1992).

² O.N.Bakharev, A.V.Dooglav, A.V.Egorov, O.B.Marvin, V.V.Naletov, M.A.Teplov, A.G.Volodin, and D.Wagener, in *Phase Separation in Cuprate Superconductors*, eds. E.Sigmund and K.A.Müller (Springer Verlag, Berlin, 1994), p.257.

³ Two samples $\text{YBa}_2\text{Cu}_3\text{O}_{6.66}$ have been studied. In a sample which has been stored three years after preparation, the Cu(2) ZFNMR signal has been seen. In a most recent one (less than a year) which has been used as a reference in the YBCO:Ni work by J.Bobroff et al. (Phys.Rev.Lett. **79**, 2117 (1997)), the Cu(2) signals A_I and B_I were not detected.

⁴ A.J.Vega, W.E.Farneth, E.M.McCarron, and R.K.Bordia, Phys.Rev.B **39**, 2322 (1989).

- ⁵ In the version "θ free" the Cu(2) ZFNMR line at a frequency of 132 MHz (see Fig.3) was assumed to be a forbidden transition of the A_I -sites.
- ⁶ J.Mesot, P.Allenspach, U.Staub, A.Furrer, and H.Mutka, Phys.Rev.Lett. **70**, 865 (1993).
- ⁷ M.Iliev, C.Thomsen, V.Hadjiev, and M.Cardona, Phys.Rev.B **47**, 12341 (1993).
- ⁸ O.N.Bakharev, A.V.Dooglav, A.V.Egorov, E.V.Krjukov, Yu.A.Sakhratov, and M.A.Teplov, JETP Lett. **64**, 398 (1996).
- ⁹ O.N.Bakharev, L.K.Aminov, A.V.Dooglav, A.V.Egorov, E.V.Krjukov, I.R.Mukhamedshin, V.V.Naletov, M.A.Teplov, A.G.Volodin, J.Witteveen, H.B.Brom, and H.Alloul, Phys.Rev.B **55**, 11839 (1997).
- ¹⁰ J.M.Tranquada, P.M.Gehring, G.Shirane, M.Sato, and S.Shamoto, Phys.Rev.B **46**, 5561 (1992).
- ¹¹ B.J.Sternlieb, J.M.Tranquada, G.Shirane, M.Sato, and S.Shamoto, Phys.Rev.B **50**, 12915 (1994).
- ¹² J.M.Tranquada. Charge stripes and spin correlations in copper-oxide superconductors, cond-mat/9702117.
- ¹³ P.Dai, H.A.Mook, and F.Dogan. Incommensurate magnetic fluctuations in $\text{YBa}_2\text{Cu}_3\text{O}_{6.6}$, cond-mat/9707112.
- ¹⁴ J.M.Tranquada, B.J.Sternlieb, J.D.Axe, Y.Nakamura, and S.Uchida, Nature **375**, 561 (1995); J.M.Tranquada, J.D.Axe, N.Ichikawa, Y.Nakamura, S.Uchida, and B.Nachumi, Phys.Rev.B **54**, 7489 (1996).
- ¹⁵ J.M.Tranquada, J.D.Axe, N.Ichikawa, A.R.Moodenbaugh, Y.Nakamura, and S.Uchida, Phys.Rev.Lett **78**, 338 (1997).
- ¹⁶ O.N.Bakharev, M.V.Eremin, and M.A.Teplov, JETP Lett. **61**, 515 (1995).
- ¹⁷ J.L.Tallon, C.Bernhard, H.Shaked, R.L.Hitterman, and J.D.Jorgensen, Phys.Rev.B **51**, 12911 (1995).
- ¹⁸ S.Yang, H.Claus, B.W.Veal, R.Wheeler, A.P.Paulikas, and J.W.Downey, Physica C **193**, 243 (1992).
- ¹⁹ P.Schleger, H.Casalta, R.Hadfield, H.F.Poulsen, M.von Zimmermann, N.H.Andersen, J.R.Schneider, R.Liang, P.Dosanjh, and W.N.Hardy, Physica C **241**, 103 (1995).

VI. FIGURE CAPTIONS

Fig.1. Tm and Cu(2) NMR spectra of the aligned Tm_{6+x} powders with $x=0.51$ (triangles), 0.6 (light circles), 0.7 (squares) at a frequency of 70 MHz in an external field H perpendicular to the c -axis. Cu(2) NMR is particularly pronounced in the saturated spectrum of Tm_{6.6} (black circles) taken at a pulse sequence repetition rate of $F=100$ Hz. Inset: ac diamagnetic susceptibility of Tm_{6+x} at liquid helium temperature (frequency of 1 kHz, $H_1 \approx 1$ Oe); circles - for 1-year aged samples², crosses - for 6-years aged samples.

Fig.2. Copper NQR spectra of Tm_{6.6} at a temperature of 4.2K: (a) non-saturated Cu(1) and Cu(2) spectra ($F=1$ Hz), (b) saturated Cu(1) and Cu(2) spectra ($F=200$ Hz), (c) ratio of the non-saturated to saturated echo intensity, (d) Cu(2) NQR spectrum, (e) Cu(1) NQR spectrum. Solid line in (d) is an approximation by four Gaussians (for parameters see Table I).

Fig.3. Cu(2) ZFNMR spectra of (a) Tm_{6.51}, (b) Tm_{6.6}, (c) Tm_{6.7} and (d) Y_{6.66} at a temperature of 4.2K. Black squares in (b) is the spectrum at $T=77$ K multiplied by a factor of 10. The YBa₂Cu₃O_{6.66} sample was stored at room temperature for 3 years after preparation.

Fig.4. Calculated Cu(2) NQR and ZFNMR spectra of (a) Tm_{6.51}, (b) Tm_{6.6}, (c) Tm_{6.7} and (d) Y_{6.66} obtained from the experimental spectra of Fig.3 as a superposition of six Gaussians: solid lines $F_0(\nu)$ - taking into account the ν^2 -type dependence of the spin-echo intensities and the losses of signal intensities due to spin-spin relaxation, dotted lines $F_{2\tau}(\nu)$ - taking into account the ν^2 -dependence only (for details see text). The integrated intensities of the S_I - and S_{II} -spectra depicted by solid lines are normalized by the intensity of the Cu(2) ZFNMR spectrum of the 1 gram TmBa₂Cu₃O_{6.1} sample at $T=4.2$ K. For convenience of comparison, the ZFNMR spin-echo intensities are multiplied by a factor of 15.

Fig.5. Cu(2) ZFNMR spectra of (a) Tm_{6.51} and (b) Tm_{6.6} obtained from the experimental spectra of Figs.3a,b by taking into account the losses of signal intensities due to spin-spin relaxation (for details see text). Solid lines in (a) and (b) represent the results of the numerical diagonalization of the two Hamiltonians with the parameters given in Eqs.(1),(2),(3),(4); solid line in (c) represents the spectrum of Tm_{6.6} calculated with the parameters given in Eqs.(5), (6).

Fig.6. Plausible stripe patterns in the (a) optimally doped ($p = 1/6$ hole per Cu(2)) and (b) underdoped ($p = 1/9$) CuO₂ planes. Copper atoms carrying magnetic moments of opposite orientations are shown by big light and black circles, those carrying no magnetic moments are shown by small circles, solid lines mark the centers of the non-magnetic (hatched) and magnetic (non-hatched) stripes. The period of 18 lattice spacings of the magnetic superstructure in (b) is twice as large as the period of the charge pattern.

Sample	Site	$^{63}\nu_Q$ (MHz)	Full rms width (MHz)	Intensity
Tm6.51	<i>A_{II}</i>	29.44(2)	1.35(3)	0.65(1)
	<i>B_{II}</i>	26.76(6)	1.17(4)	0.35(4)
Tm6.6	<i>A_{II}</i>	29.69(2)	1.75(4)	0.69(1)
	<i>B_{II}</i>	27.01(6)	1.46(4)	0.31(4)
Tm6.7	<i>A_{II}</i>	30.36(3)	2.02(6)	0.68(1)
	<i>B_{II}</i>	27.39(6)	1.79(9)	0.32(2)

TABLE I. Parameters of the $^{63}\text{Cu}(2)$ NQR spectra (type *II*) in Tm6+x samples at T=4.2K (with no corrections for the frequency dependence and for the spin-spin relaxation time T_2)

Sample	ZFNMR S_{AI}/S_{BI}		NQR S_{AII}/S_{BII}		NQR/ZFNMR S_{II}/S_I
	Lorentzian approximation with the T_2 corrections	Gaussian approximation with the T_2 corrections	Gaussian approximation with no T_2 corrections	Gaussian approximation with the T_2 corrections	Gaussian approximation with the T_2 corrections
Tm6.51	1.6(3)	1.6(4)	1.8(2)	1.8(6)	0.791/0.207=3.8(1.3)
Tm6.6	2.0(2)	2.0(5)	2.2(2)	2.0(7)	0.424/0.154=2.8(9)
Tm6.7		3.7(1.2)	2.1(2)	2.5(9)	0.725/0.104=7(2)
Y6.66		3.3(1.2)	2.6(9)	3.8(1.3)	3.7(1.3)

TABLE II. Intensities of the Cu(2) spectra in Tm6+x (x=0.51, 0.6, 0.7) and Y6.66 at T=4.2K

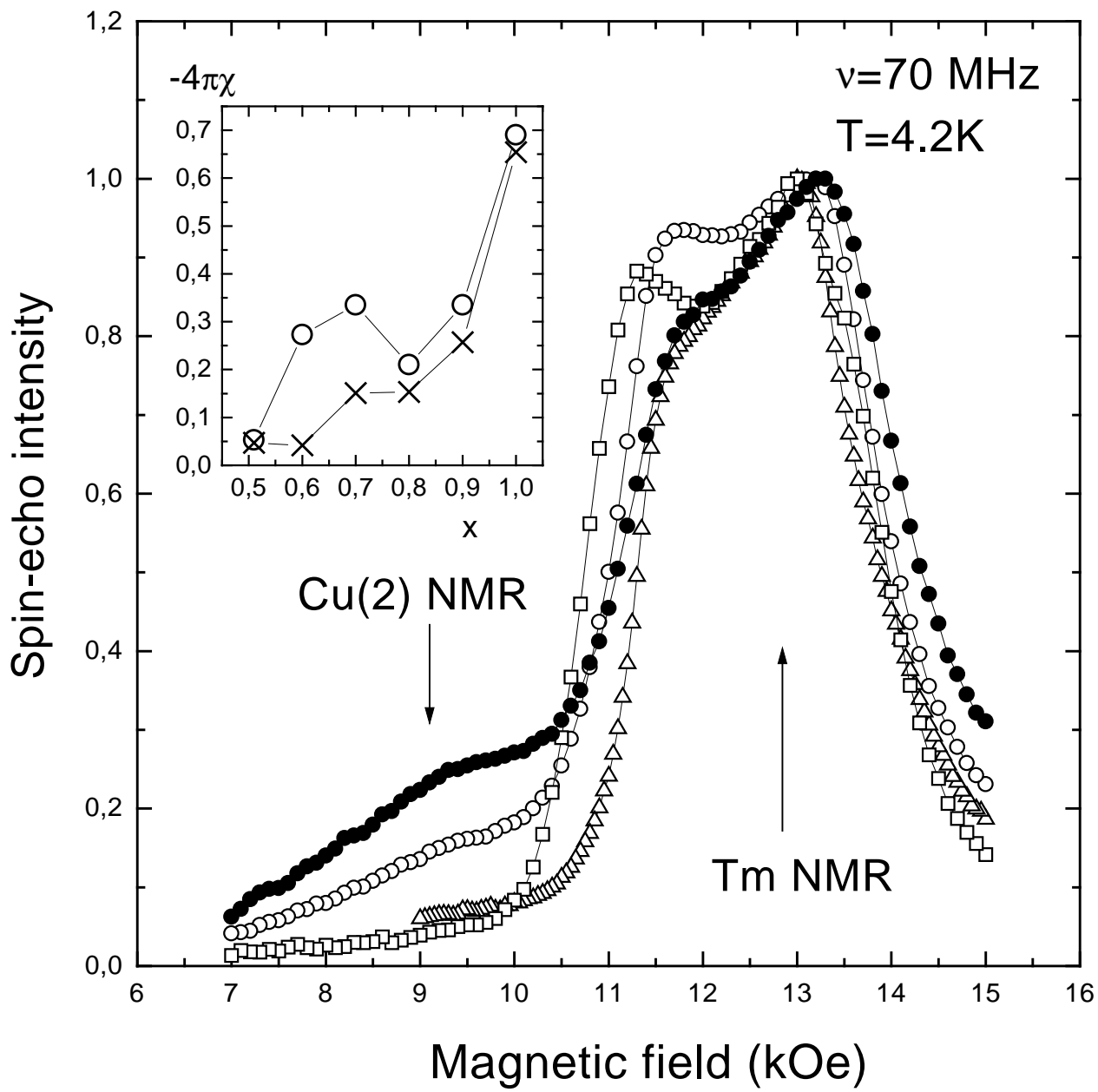


Fig.1

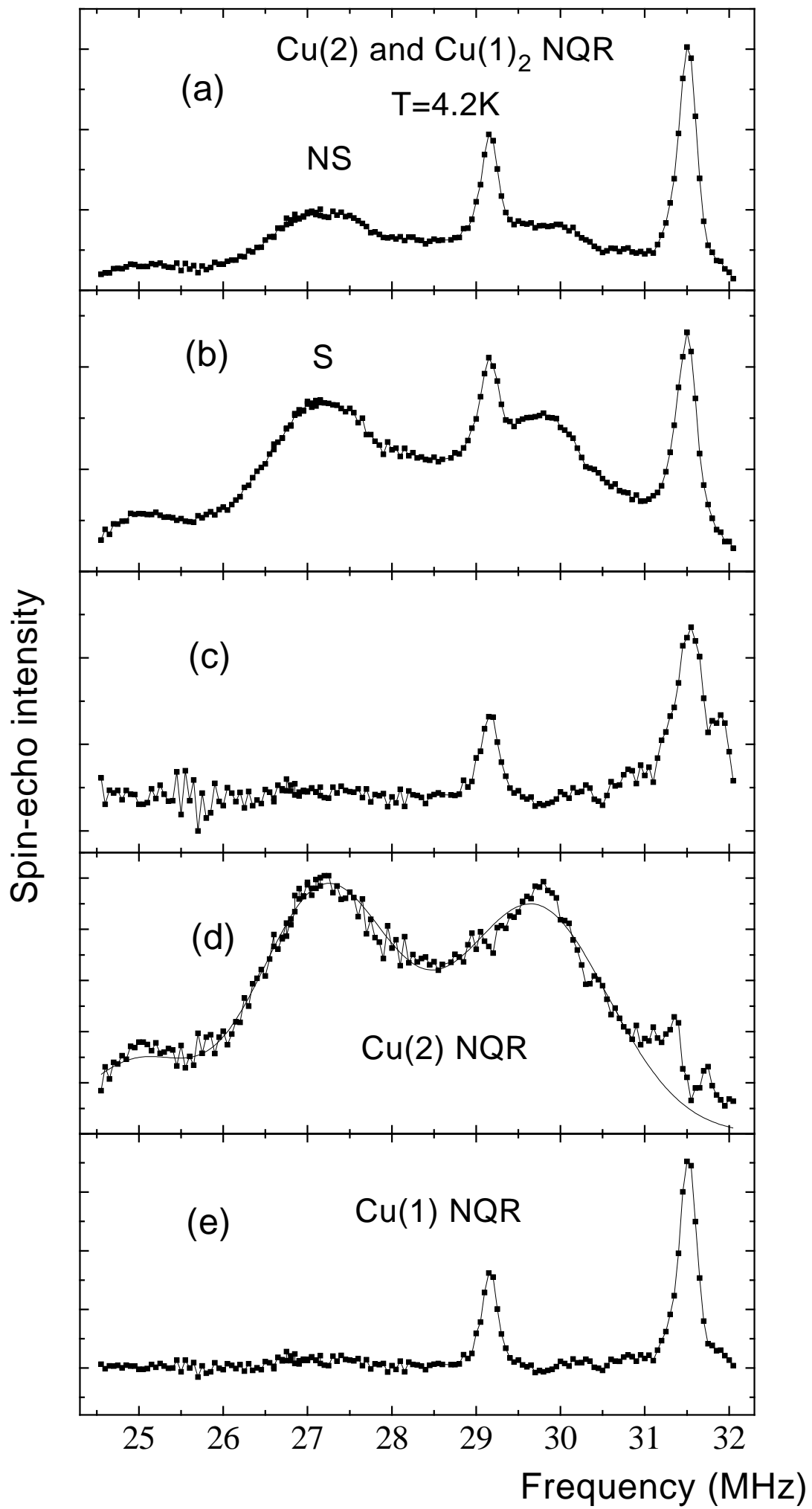


Fig.2

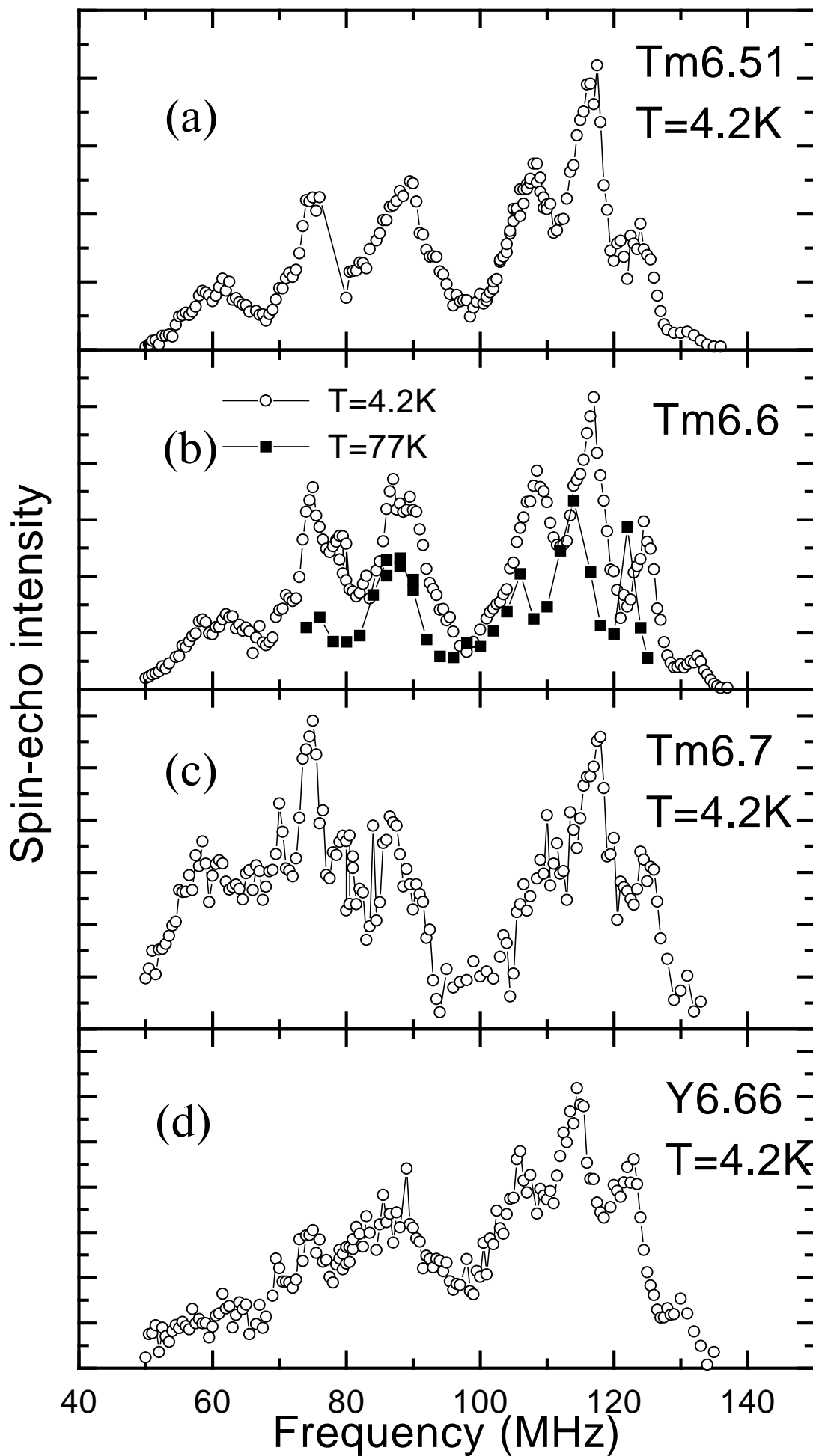


Fig.3

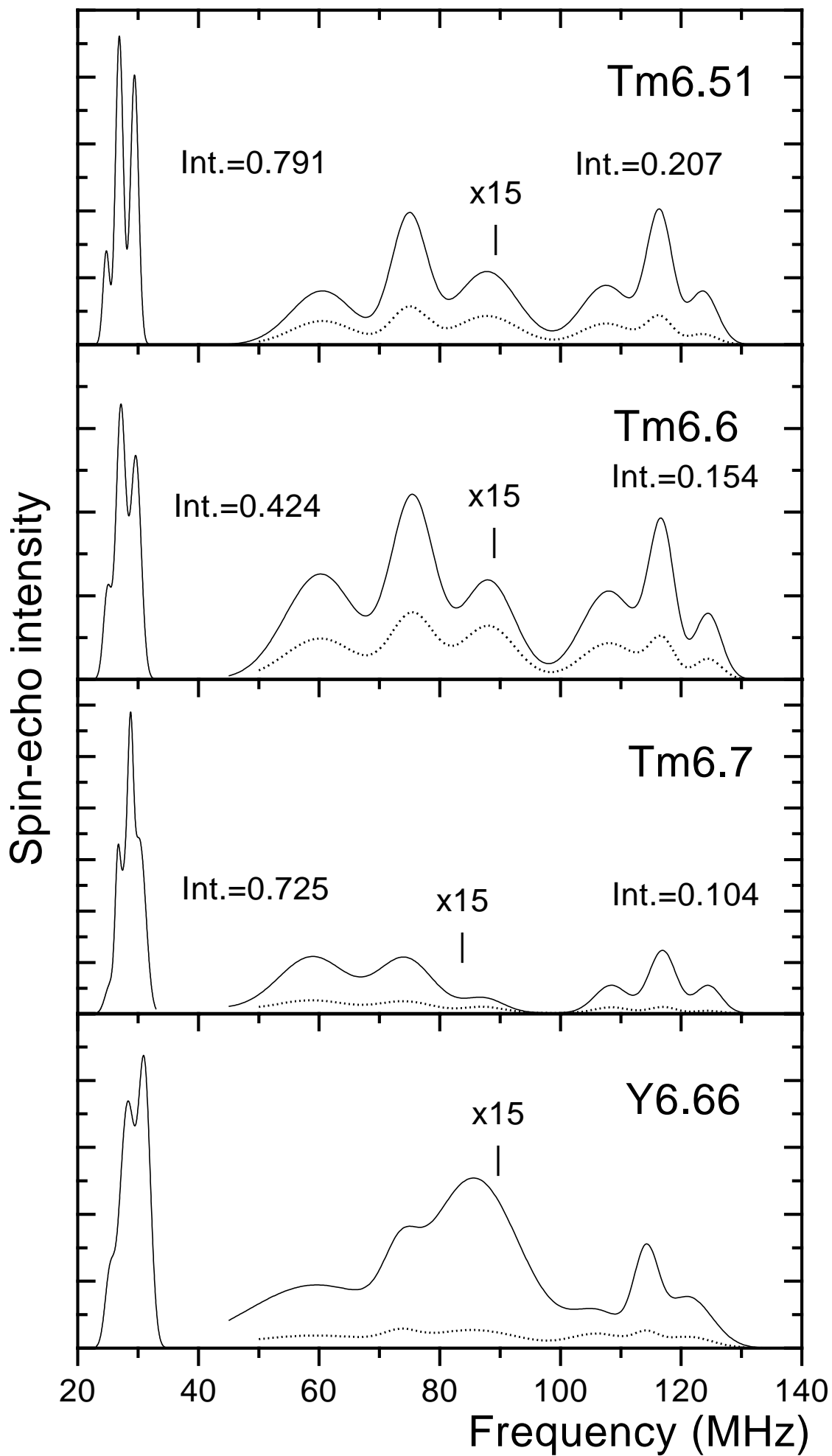


Fig.4

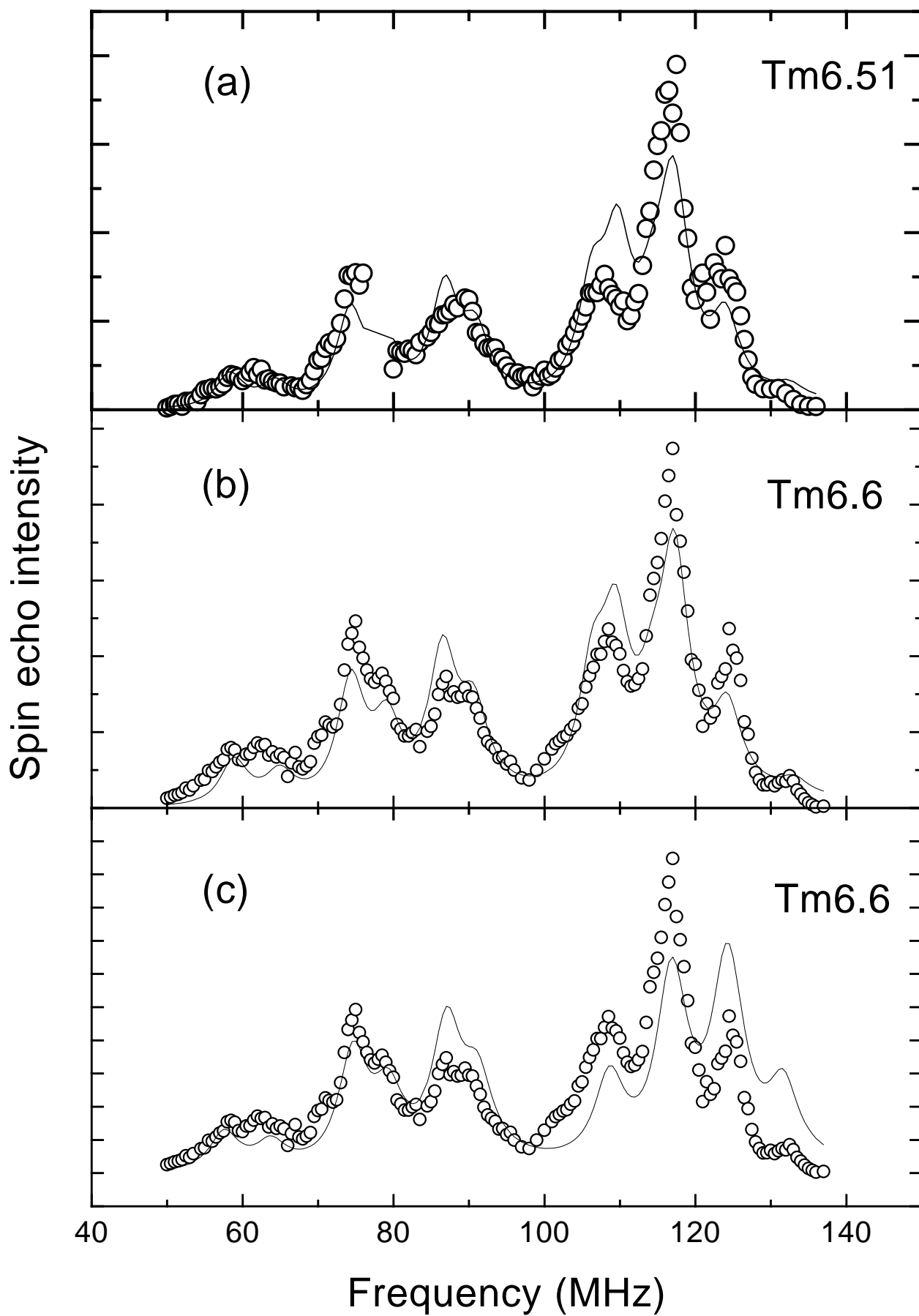


Fig.5

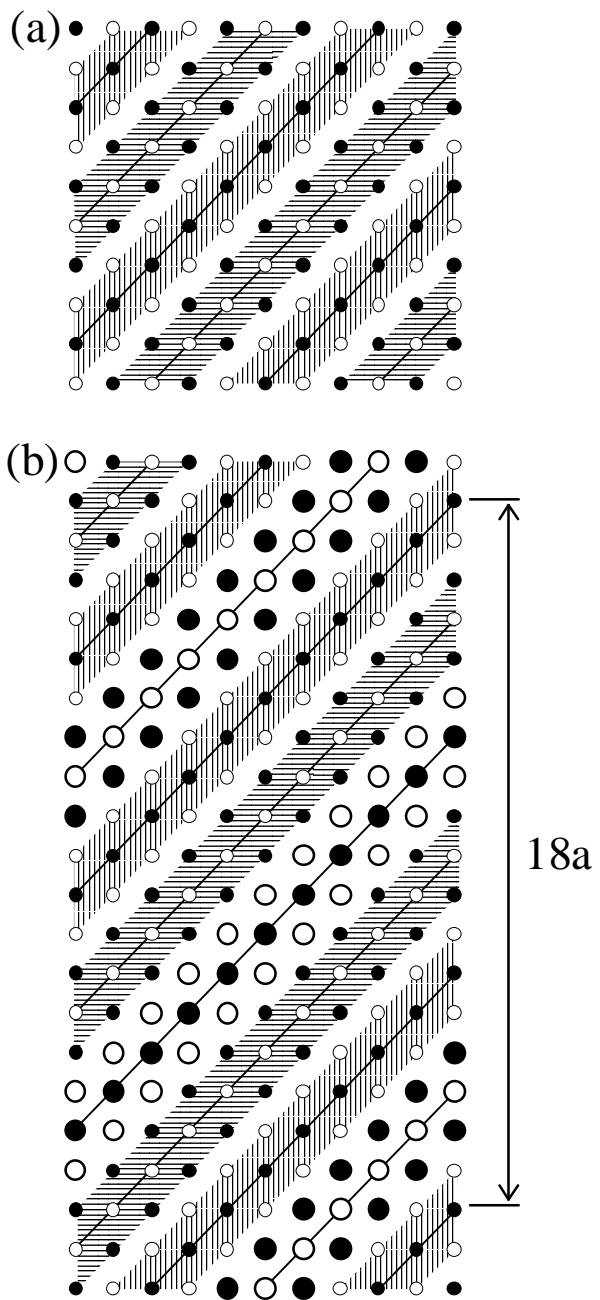


Fig. 6